Int. J. Heat Mass Transfer. Vol. 12, pp. 1–13. Pergamon Press 1969. Printed in Great Britain

FLOW AND HEAT-TRANSFER MEASUREMENTS IN SUBSONIC AIR FLOW THROUGH A CONTRACTION SECTION†

L. H. BACK,‡ P. F. MASSIER§ and R. F. CUFFEL‖
Jet Propulsion Laboratory, Pasadena, California, U.S.A.

(*Received* 13 *November* 1967 *and in revised form* 19 *March* 1968)

Abstract—Flow and heat-transfer measurements are presented for heated air flowing subsonically through a contraction section smoothly connecting a tube to a conical section. These measurements spanned a range of cooled wall-to-stagnation temperature ratios, T_w/T_{to}, from $\frac{1}{3}$ to $\frac{2}{3}$, Reynolds numbers from 2×10^4 to 2×10^5, with data obtained for both laminar and turbulent boundary layers. Unheated air flow measurements were also made. The basic flow field established from measurements along the wall and centerline consists of a turning of the flow through the contraction section that resulted in an adverse pressure gradient (deceleration) along the wall. Flow-visualization results indicated that the flow separated just upstream of the curved contraction section and reattached near its end. The heat-transfer coefficients reached a minimum value near the center of the separation region, increased in the vicinity of the reattachment point, flattened out in the reattachment region, and then increased again downstream. As a consequence of the curved section and the associated separated flow effects, the heat transfer in the separation region under certain operating conditions was reduced below values measured upstream in the tube. Values of the heat-transfer coefficient were higher with thin boundary layers produced by a short, cooled upstream length, and the distribution of the heat-transfer coefficient in the redevelopment region depended on whether the boundary layer was turbulent or laminar. Effects of wall cooling in terms of T_w/T_{to} that were found upstream in the tube were not observable in the separation and reattachment regions.

NOMENCLATURE

- D, diameter;
- h, convective heat-transfer coefficient;
- k, thermal conductivity;
- l, length of cooled tube;
- L, unit length, 1 in.;
- M, Mach number;
- p, static pressure;
- p_t, stagnation pressure;
- Pr, Prandtl number;
- r, radius;
- R, tube radius;
- T, temperature;
- u, velocity component along wall;
- y, distance normal to wall;
- z, axial distance from curved inlet.

Greek symbols

- γ, specific heat ratio;
- δ, velocity boundary layer thickness;
- δ_t, thermal boundary layer thickness;
- δ^*, displacement thickness,

$$\delta^* \left(R - \frac{\delta^*}{2}\right) = \int_0^\infty \left(1 - \frac{\rho u}{\rho_e u_e}\right)(R - y)\,dy;$$

† This work presents the results of one phase of research carried out at the Jet Propulsion Laboratory, California Institute of Technology, under Contract No. NAS7-100, sponsored by the National Aeronautics and Space Administration.

‡ Senior Engineer, Propulsion Research and Advanced Concepts Section.

§ Group Supervisor, Propulsion Research and Advanced Concepts Section.

‖ Senior Engineer, Propulsion Research and Advanced Concepts Section.

θ, momentum thickness,

$$\theta\left(R-\frac{\theta}{2}\right) = \int_0^\infty \frac{\rho u}{\rho_e u_e}\left(1-\frac{u}{u_e}\right)(R-y)\,dy;$$

μ, viscosity;
ρ, density;
ϕ, energy thickness,

$$\phi\left(R-\frac{\phi}{2}\right) = \int_0^\infty \frac{\rho u}{\rho_e u_e}\left[1-\left(\frac{T-T_w}{T_e-T_w}\right)\right](R-y)\,dy.$$

Subscripts

c_L, centerline;
e, condition at free-stream edge of boundary layer;
i, condition upstream in tube;
o, upstream reservoir condition;
ref, reference condition;
t, stagnation condition;
w, wall condition.

INTRODUCTION

SUBSONIC flows through channels that have contraction sections are of interest in acceleration devices such as wind tunnels and rocket nozzles, and in connection with flowmeters, reducer fittings in pipelines, etc. Treating these flows on a one-dimensional basis, the average fluid velocity for steady flow must increase through the contraction to satisfy the continuity equation for low-speed flow, where the density variation is negligible. However, a fluid flowing from a channel of constant cross-sectional area and into a contraction section can experience a more complicated behavior as has been known for many years, particularly in the design of wind tunnels. As a result of being turned by the channel wall, the fluid near the wall can be locally decelerated, while the fluid near the centerline can be accelerated. The adverse pressure gradient accompanying flow deceleration along the wall can influence the shear flow near the wall and local flow separation may occur.

The purpose of this paper is to present some flow and heat-transfer measurements in an axisymmetric contraction section through which heated air flowed. Previous heat-transfer investigations in supersonic axisymmetric nozzles were not of sufficient detail in the curved inlet section [1, 2] to provide local heat-transfer measurements. In this investigation, the wall was cooled externally and semi-local heat-flux measurements were obtained by calorimetry in individual circumferential coolant passages, with passage widths relatively small compared to the radius of the curved-wall contraction section. Pitot tube and temperature surveys were made upstream of the curved section to determine the boundary-layer structure (laminar or turbulent) and the thickness of the layer. Conditions along the wall were obtained from wall static-pressure measurements and flow-visualization results. Conditions along the centerline were established with unheated air by traversing a small tube (0·036 in. in diameter), which extended through the entire nozzle and into the upstream tube, with a 0·006-in dia. hole on its side, through which the static pressure was measured. Heat-transfer data are presented for both laminar and turbulent boundary layers.

The contraction section formed the inlet of a supersonic nozzle that was operated at a choked condition over a range of stagnation pressures from 30 to 250 lb/in and heated air stagnation temperatures from 1000 to 2000°R. Heat-transfer coefficients were calculated from the measured wall heat fluxes and differences between adiabatic wall and cooled wall temperatures, except in separated flow regions where differences between stagnation temperature and wall temperature were used. The heat-transfer coefficients reported are believed to be accurate to within 10 per cent. The ratio of cooled wall temperature-to-stagnation tempera-

ture ranged from $\frac{1}{3}$ to $\frac{2}{3}$. Reference [3] presents additional information on the test apparatus and measurement technique.

The flow regimes characterized by the measurements involve the effect of adverse pressure gradients on both laminar and turbulent boundary layers with wall cooling, apparent separation and reattachment of the flow, and subsequent redevelopment of the flow downstream in an acceleration region.

RESULTS

Figure 1 shows the curved contraction section formed by the intersection of a 2·5-in radius tube and a 45° half-angle conical section. A circular-arc section of 0·80-in radius of curvature smoothly joins the tube to the conical section. The flow field under consideration is indicated by the static pressure measurements from which Mach numbers were calculated for isentropic flow of unheated air ($\gamma = 1{\cdot}4$) from the stagnation pressure measured upstream of the contraction to the static pressures indicated. The influence of the contraction section on the flow through the tube extends approximately 3·5 in upstream of the curved inlet. At this upstream location, the static pressure along the wall (open symbols) begins to increase

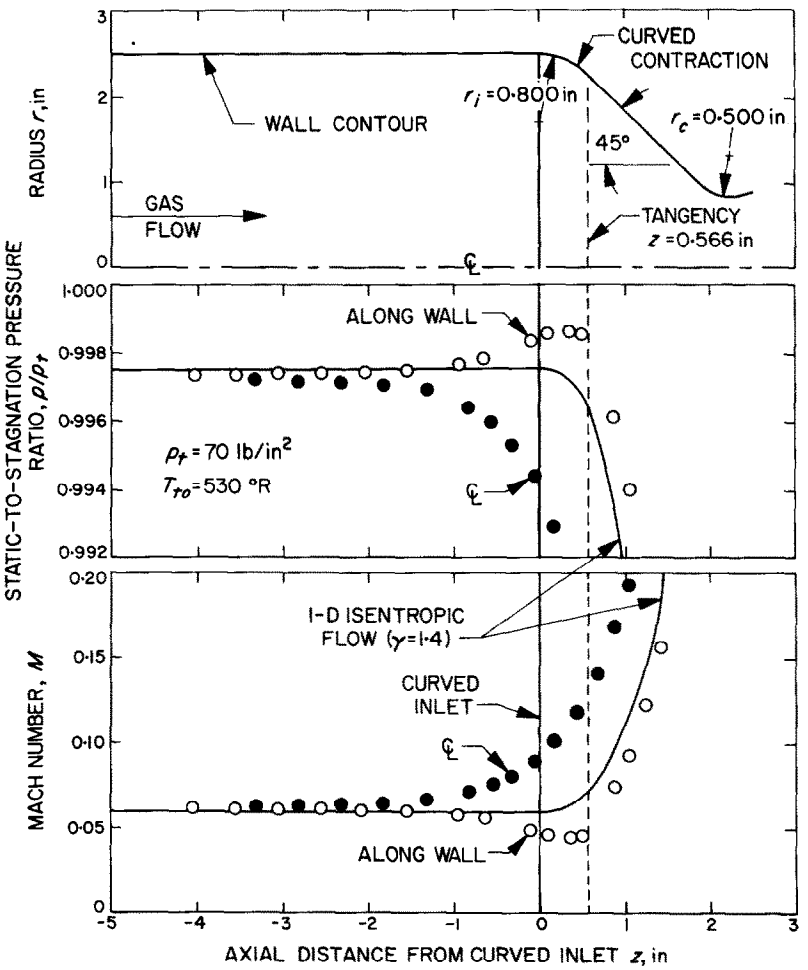

FIG. 1. Ratio of static-to-stagnation pressure and Mach number along the centerline and wall.

(adverse pressure gradient), while the static pressure along the centerline (shaded symbols) starts to decrease. In this region, differences between static pressure and upstream stagnation pressure were read on water manometers. The magnitude of the measured pressure rise along the wall amounted to 2·3 in of water. The static pressure along the wall continues to rise through the curved section, apparently reaching a maximum within this section; it then decreases downstream. Correspondingly, the Mach number along the wall decreases by 25 per cent from the upstream value of 0·061, determined by the contraction area ratio of the nozzle, to a value of 0·045; it then increases further downstream. The velocity variation is virtually the same as that of the Mach number in this low-speed region. A prediction for one-dimensional isentropic flow is shown as a reference curve to illustrate the large deviations that exist. Along the centerline, the velocity increases monotonically, so that, in the curved section, the Mach number along the centerline exceeds the value along the wall by a factor as large as 2·5.

A flow visualization study was made for the conditions shown in Fig. 1 by bleeding a small amount of ammonia gas through the wall pressure tap holes. Ammonia-sensitive paint was applied to the gas side wall in the vicinity of the pressure tap holes. The wall streaks observed are indicative of flow direction, as shown in Fig. 2 in an artist's rendition of the results, and local separation occurred approximately 0·25 in upstream of the curved inlet. The flow reattached near the end of the curved inlet section, approximately 0·45 in downstream of the curved inlet. For this test, a pitot tube traverse at a distance $z = -1{\cdot}7$ in upstream in the 9·1-in long tube, indicated the boundary layer to be turbulent with thickness approximately 0·05 of the tube radius and momentum thickness Reynolds number of 2100. As a result of the boundary-layer displacement effect, the Mach number upstream in the tube, where the effect of the contraction is negligible, is

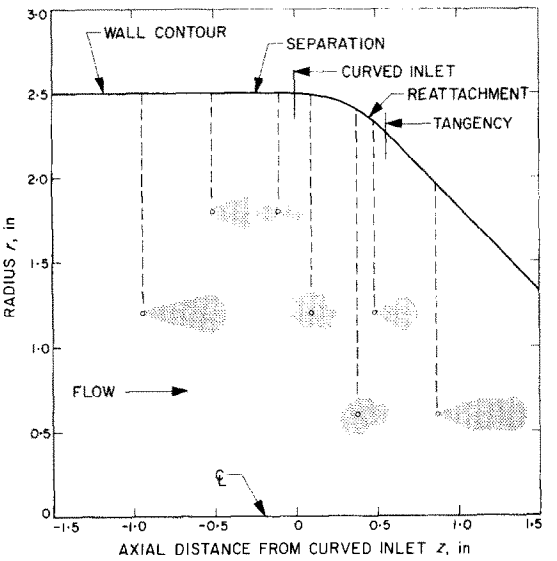

FIG. 2. Flow-visualization results.

slightly higher than the one-dimensional isentropic flow value shown in Fig. 1.

Unheated air tests were made at lower and higher stagnation pressures than the 70 lb/in^2 test shown in Fig. 1. These tests, which spanned stagnation pressures from 30 to 150 lb/in^2, revealed essentially the same pressure ratio and Mach number distribution along the wall, as shown in Fig. 1. As a result of measurement accuracy, these data showed some scatter; however, there were no trends indicating any dependence on Reynolds number. It should be recalled that, for choked operation, the mass flow rate and, therefore, the Reynolds number are proportional to the stagnation pressure.

With the flow field established, the air was heated at a remote distance upstream by combustion of a small amount of methanol introduced through a spray nozzle. Combustion effects were minimized by separating the combustion chamber from the test section with a large calming chamber which contained baffles to promote mixing, and screens at the exit to reduce large-scale turbulence. Downstream of the calming section, the flow accelerated in a gradual contraction section of area ratio

11·6 before entering a tube that was cooled over part of its length. Two cooled approach lengths were employed, one was 43-in long and the other 1·35 in. In terms of tube diameters, the corresponding l/D ratios are 8·6 and 0·27.

Figure 3 illustrates the results obtained with the longer cooled tube at a nominal stagnation temperature of 1500°R and over a range of stagnation pressures from 30 to 250 lb/in^2. Velocity and temperature profiles are shown at the highest stagnation pressure to indicate the nature of the flow in the tube upstream of the curved section. The velocity profile, when plotted in the usual representation with distance from the wall normalized by the momentum thickness, coincides with a $\frac{1}{7}$ power profile typical of a turbulent boundary layer. This correspondence was found over the entire stagnation pressure range, so that, for the results shown in Fig. 3, the boundary layer was turbulent upstream of the curved section. The temperature distribution is similar to the velocity distribution when normalized to the wall and free-stream values in the usual way. Tabular values of thicknesses associated with the boundary layer are indicated in the table of Fig. 3. The momentum thickness was nearly the same over the stagnation pressure range so that the momentum thickness Reynolds numbers, which vary from approximately 2000 to 18000 (typical of turbulent boundary layers), reflect the dependence of mass flux on stagnation pressure for choked nozzle flow. The effect of wall cooling is to decrease the ratio of displacement-to-momentum thickness, δ^*/θ, below a value of approximately 1·3 associated with constant-property turbulent-boundary layers with constant free-stream velocity. Values of δ^*/θ tabulated are less than 0·5. Compared to the tube radius, the displacement thickness amounted to less than 2 per cent. Values of the ratio of the energy thickness to the momentum thickness, ϕ/θ, are somewhat larger than unity, with a typical value of approximately 1·3. If the velocity boundary-layer thickness δ is estimated at ten times the momentum thickness, values of δ of approximately 45 per cent of the tube radius are obtained. The thermal layer thickness δ_t exceeds δ by approximately 30 per cent if it is defined in a similar manner, but in terms of ϕ rather than θ. This relative relation between δ and δ_t would be expected for air ($Pr = 0{\cdot}7$) if both the velocity and temperature boundary layers originated at the same location, the wall were isothermal, and the free-stream velocity variation were negligible. This situation was nearly realized for the flow through the cooled tube.

Proceeding in the flow direction, heat-transfer coefficients shown in Fig. 3 increase slightly in the cooled tube (passage T-2) before decreasing near the inlet of the curved section. The magnitude of this decrease is larger at the higher stagnation pressures or Reynolds numbers, amounting to approximately $\frac{1}{3}$ of the upstream value for the highest Reynolds number test. This decrease in the heat-transfer coefficient diminishes in magnitude at the lower Reynolds numbers, and is not found for the lowest Reynolds number test. Except for the lowest Reynolds number test, the heat-transfer coefficient reaches a minimum value in the first part of the curved section (passage C-1). The heat-transfer coefficient then increases along the curved section before beginning to flatten out just downstream of the tangency between the curved and conical sections (passage C-4). The location where this flattening out occurs appears to be shifted downstream at the lower Reynolds numbers. Still further downstream, the heat-transfer coefficient increases again along the conical section.

It is of interest to compare the variation of the heat-transfer coefficient, shown in Fig. 3 in the curved section and conical section just downstream of the tangency, to trends that have been found in separated flow regions. For example, downstream of backward facing steps [4–6] the heat-transfer coefficient increases through the separation region as the reattachment point is approached, is a maximum in the vicinity of the reattachment point, and then

decreases downstream of reattachment. The heat-transfer coefficients shown in Fig. 3 however indicate a minimum value to occur near the center of the separation and there is no pronounced peak in the coefficient in the region of reattachment. Instead, the coefficients increase again through the redevelopment region in the conical section, where flow acceleration occurs, primarily as a result of increasing mass flux along the conical section.

The results shown in Fig. 3, along with tests at intermediate stagnation pressures, are shown in Fig. 4 at a few axial stations in terms of the local Nusselt number and the Reynolds number evaluated at conditions upstream in the tube. The length L in both the Nusselt and Reynolds numbers is 1 in. For passage T-2 upstream of the curved section, the dependence of the Nusselt on the Reynolds number is typical of that for turbulent flow as indicated by the following empirical relation

$$\frac{hD}{k_{\text{ref}}} = 0{\cdot}023 \left(\frac{\rho_{\text{ref}} u_e D}{\mu_{\text{ref}}}\right)^{\frac{4}{5}} Pr^{\frac{1}{3}}. \qquad (1)$$

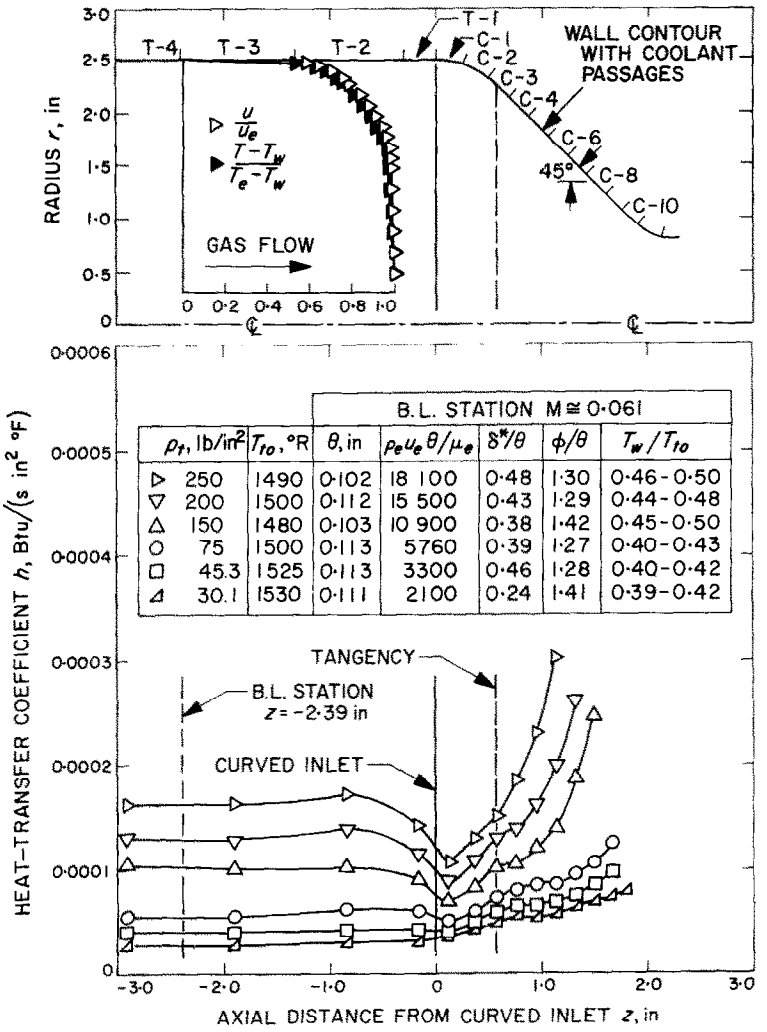

ρ_t, lb/in²	T_{to}, °R	θ, in	$\rho_e u_e \theta/\mu_e$	δ^*/θ	ϕ/θ	T_w/T_{to}
▷ 250	1490	0·102	18 100	0·48	1·30	0·46-0·50
▽ 200	1500	0·112	15 500	0·43	1·29	0·44-0·48
△ 150	1480	0·103	10 900	0·38	1·42	0·45-0·50
○ 75	1500	0·113	5760	0·39	1·27	0·40-0·43
□ 45·3	1525	0·113	3300	0·46	1·28	0·40-0·42
◿ 30·1	1530	0·111	2100	0·24	1·41	0·39-0·42

FIG. 3. Heat-transfer coefficients with a turbulent boundary layer and cooled approach length of 43 in.

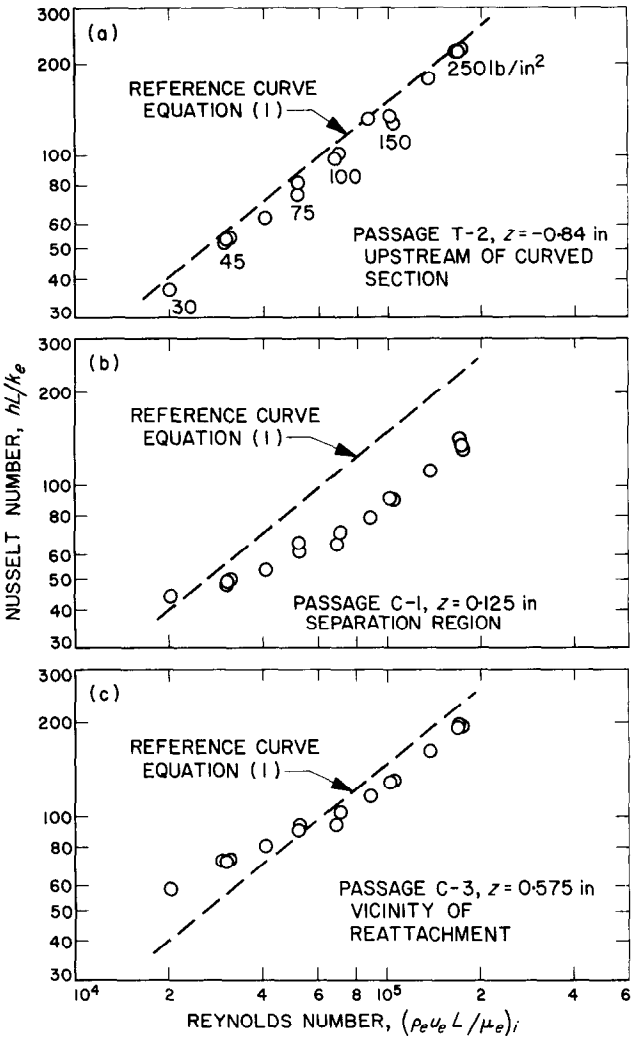

FIG. 4. Nusselt numbers at various axial locations with a turbulent boundary layer and cooled approach length of 43 in.

In applying equation (1), the properties ρ_{ref}, μ_{ref}, and k_{ref} were evaluated with the stagnation temperature chosen as the reference temperature, and the Reynolds number based on the tube diameter D was evaluated at conditions upstream in the tube. Equation (1), associated with fully developed constant property flow through a tube, is shown herein as a reference curve and does not imply that the variable property flow was fully developed after 8·6 diameters of cooled length. However, the flow may have been fairly close to a quasi-fully developed condition and, to bring equation (1) in line with the results, a lower value of the coefficient 0·023 would be needed. In the first part of the curved section, passage C-1, where the heat-transfer coefficient is a minimum and the flow separated, the Nusselt number variation is no longer describable on a power law basis over the Reynolds number range. At the lower

Reynolds numbers, less than a $\frac{4}{5}$ power dependence on Reynolds number is evident. Further downstream in passage C-3, at the tangency between the curved and conical sections and just downstream of the reattachment indicated by the test shown in Fig. 2, the Nusselt number variation with Reynolds number is similar in shape to that at passage C-1, but the Nusselt number is higher, as would be expected, in the vicinity of reattachment. A conservative

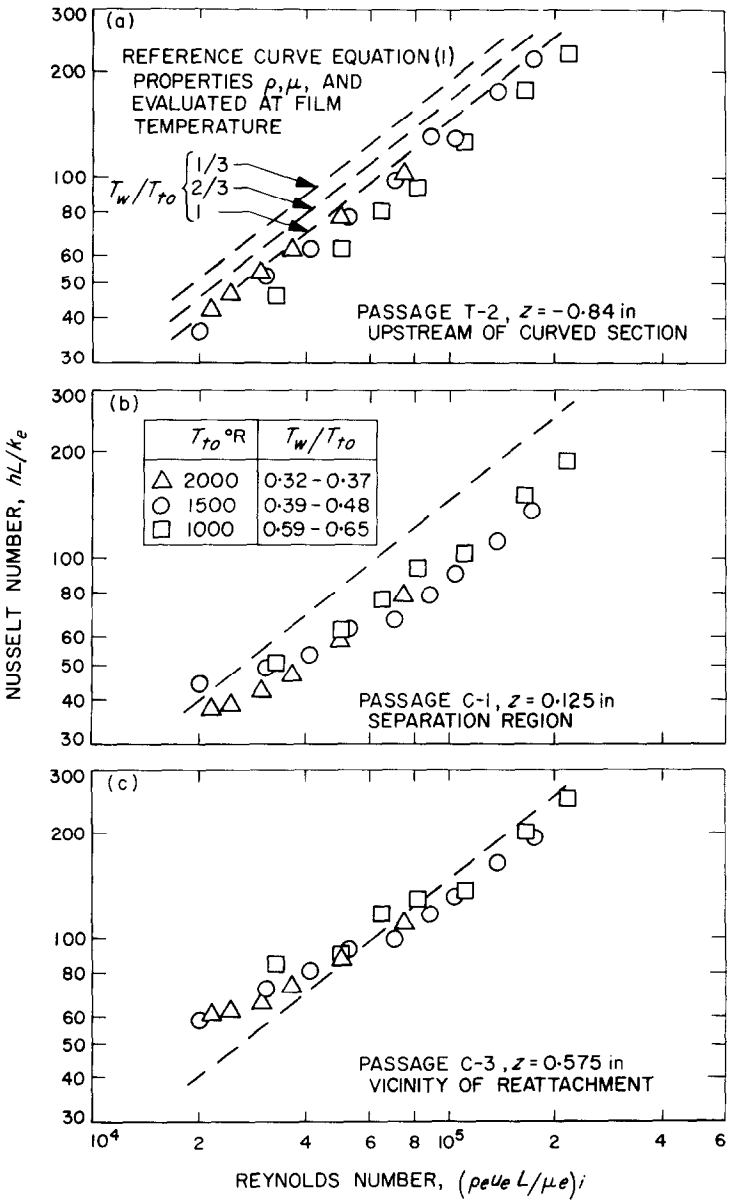

FIG. 5. Effect of wall cooling T_w/T_{to} on the Nusselt number at various axial locations with a turbulent boundary layer and cooled approach length of 43 in.

estimate of the Nusselt number in the curved inlet region is provided by equation (1) at the higher Reynolds numbers for turbulent flow when both the velocity and thermal boundary layers are relatively thick upstream in the tube. However, this situation is not found at the lower Reynolds numbers where the data lie above the reference curve.

The results from Fig. 4 at a nominal stagnation temperature of 1500°R are shown in Fig. 5 along with data obtained at lower and higher stagnation temperatures of 1000 and 2000°R. The purposes of experimentally varying the stagnation temperature on the Nusselt–Reynolds number relation is primarily to determine whether there is any influence of variable properties over the range of wall-to-stagnation temperature ratios T_w/T_{to} from $\frac{1}{3}$ to $\frac{2}{3}$. In the representation of the data shown in Fig. 5, properties in the Nusselt and Reynolds numbers were evaluated at the stagnation condition. Upstream of the curved section there is a dependence on T_w/T_{to}, with the Nusselt number at a given Reynolds number increasing with the amount of wall cooling; i.e. decreasing T_w/T_{to}. Taking the viscosity and thermal conductivity proportional to T^{ω}, the effect of evaluating properties ρ, μ and k in equation (1) at the film temperature is shown in Fig. 5 for $\omega = 0{\cdot}7$, which is a good approximation of the actual variation of μ and k for air over the temperature range of interest. These predictions indicate the same trend with T_w/T_{to} that is exhibited by the data, although a selection of a lower value for the constant 0·023 would improve the correspondence with the data upstream of the curved section as previously mentioned. In the separation and reattachment regions downstream, however, the upstream dependence on T_w/T_{to} is no longer observable. The reference curve shown at these locations is the same as that shown in Fig. 4, and the data display the same trends relative to this curve, as discussed previously in connection with Fig. 4.

The results presented so far were obtained with the long, cooled tube. Data acquired with the short, cooled tube 1·35-in long with a short uncooled upstream length of 2·5 in are shown in Figs. 6 and 7 at a stagnation temperature of 1500°R. With the short, cooled tube, both the velocity and temperature boundary-layer thicknesses were appreciably reduced below the thicker layer results, and the structure of the boundary layer depended on the operating condition, i.e. stagnation pressure. As established in the following discussion, the boundary layer was laminar upstream of the curved section at the lower stagnation pressures (Fig. 6), and was turbulent at the highest stagnation pressure (Fig. 7). Pitot tube traverses in the outer part of the rather thin boundary layer established the relative thickness of the velocity boundary layer compared to the tube radius, as indicated in the tables of Figs. 6 and 7; values of δ/R range from 0·02 to 0·04, with the lower values corresponding to the higher stagnation pressures and thus mass fluxes. However, it was not possible to determine the structure of the boundary layer from the pitot traverse in the outer part of the layer. Instead, heat-transfer measurements (to be published) in the inlet of the long tube, when attached, indicated natural transition from a laminar to a turbulent boundary layer to occur in the inlet region of the tube at the lower stagnation pressures. At the highest stagnation pressure, transition had apparently occurred upstream of the tube inlet. Since the structure of the boundary-layer upstream of the curved contraction section should be essentially the same as that at the entrance of the long tube, the boundary layer was inferred to be laminar at the lower stagnation pressures and turbulent at the highest pressure.

The heat-transfer coefficients shown in Fig. 6 for the thin laminar boundary layer exhibit similar trends upstream and in the curved section, as with the thick turbulent layers. The heat-transfer coefficients shown at the first coolant passage T-2 probably exceed the actual values that would exist if wall cooling were to begin ideally at the upstream edge of the

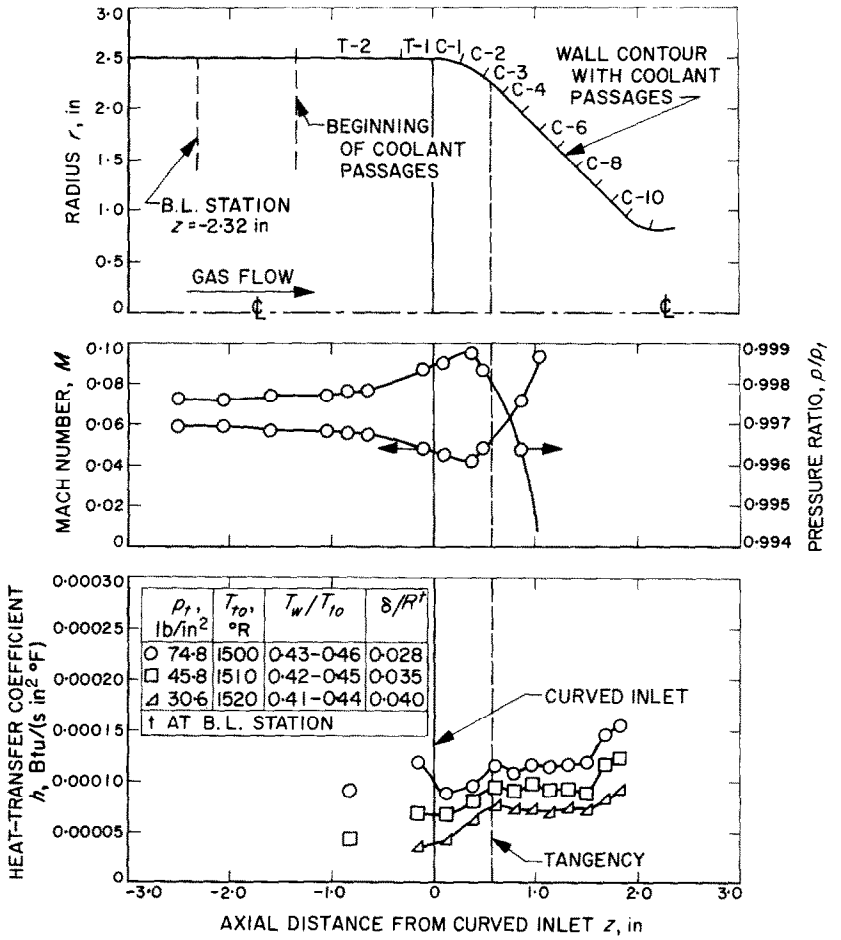

FIG. 6. Heat-transfer coefficients with a thin laminar boundary layer and a short, cooled approach length of 1·35 in.

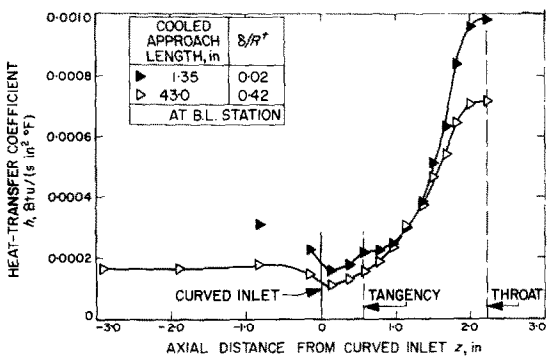

FIG. 7. Effect of thickness of the turbulent boundary layer and cooled approach length on the heat-transfer coefficient at a stagnation pressure of 250 lb/in² and stagnation temperature of 1500°R.

passage. Instead, some heat is transferred to the wall that is cooled upstream, and this heat flows into the first coolant passage by conduction along the wall. Therefore, the precise location of where cooling begins is not known, but the thermal layer thickness is considerably smaller than for the long, cooled tube results. The nature of the flow, as reflected by the variation of the heat-transfer coefficient at the end of the curved section and in the conical section, is more clearly evident with the thin laminar layer. The local peak in the heat-transfer coefficient at the tangency between the two sections indicates reattachment to occur

in the vicinity of the tangency. Whereas, for the thick turbulent layers, the heat-transfer coefficients increased again downstream of reattachment (Fig. 3), the thin laminar layer coefficients remain relatively constant an appreciable distance along the conical section. Finally, the heat-transfer coefficient again rises just upstream of the throat of the nozzle. The heat-transfer coefficients in the redevelopment region downstream of reattachment indicate that flow acceleration differently affects reattached turbulent and laminar boundary layers. For a turbulent layer, the heat-transfer coefficients increase in the redevelopment region, while for a laminar layer, they remain constant for a considerable distance along the flow acceleration region. Boundary-layer measurements in accelerated, reattached flows would be useful to learn about the basic nature of the flow, and how the competing influences of the tendency for the heat-transfer coefficient to decrease downstream of reattachment with no acceleration and to increase with acceleration interact to produce this kind of heat-transfer coefficient variation.

The effect of thickness of the boundary layer and length of the cooled tube on the heat-transfer coefficients is shown in Fig. 7 at the highest stagnation pressure where both boundary layers were turbulent. Just upstream, and in the curved section, the thin layer results (shaded symbols) exceed the thick layer results (open symbols) by approximately 50 per cent. The thin layer results then merge toward the thick layer results downstream of reattachment in the redevelopment region. Further downstream, the results again diverge, so that, in the throat region, the thin layer results exceed those of the thick layer by approximately 40 per cent.

The significant feature of the results presented for subsonic flow through a contraction section is that separation may occur with its attendant alteration of the shear flow near the wall, which is different from that which would exist without separation. The thermal resistance across the shear flow is altered and this changes the heat transfer to the wall. A more gradual turning of the flow is required to avoid separation. Attempts to analytically predict the nature of the shear flow for the conditions of these experiments are beyond the scope of this paper. This would entail the prediction of (a) the effect of adverse pressure gradients on both laminar and turbulent boundary layers with wall cooling, (b) the separation location, (c) the separation region, (d) the reattachment location, and (e) the flow development in the acceleration region downstream. Wall curvature effects would also be important in applying any conventional boundary-layer analysis to the flow under consideration. The flow considered exhibits many fluid flow regimes that have yet to be described adequately if at all, by theoretical analyses.

SUMMARY AND CONCLUSIONS

Flow and heat-transfer measurements have been presented for subsonic air flow through an axisymmetric contraction section that smoothly joined a tube to a conical section. As a result of a turning of the flow through the contraction section, an adverse pressure gradient ensues along the wall, and the heat-transfer distributions in the curved-wall section and entrance of the conical section were typical of those found in separated flow regions. The decrease in velocity along the wall amounted to approximately 25 per cent of its upstream value, and the velocity along the centerline exceeded the value along the curved section by as much as a factor of 2·5. Flow-visualization results indicated that separation occurred just upstream of the inlet of the curved section, and reattachment occurred near the end of the curved inlet section.

The heat-transfer coefficients generally decreased just upstream of the curved section, reached a minimum value in the entrance of the curved section, and then increased along the curved section. The coefficients then flattened out downstream of the tangency between the

curved and conical sections; further downstream in the conical section, the coefficients increased again when the boundary layer was turbulent. The magnitude of the heat-transfer coefficient depended on the length of upstream cooled tube and boundary-layer thickness and structure, with data presented for both laminar and turbulent boundary layers. As expected, the heat-transfer coefficients were higher with a short, cooled length of tube. For a turbulent layer, the heat-transfer coefficients increased in the redevelopment region downstream of reattachment and in the flow acceleration region, while for a laminar layer, they remained constant in the redevelopment region a considerable distance downstream. The effect of property variation found upstream in the tube as a result of cooled wall-to-stagnation temperature ratios from $\frac{1}{3}$ to $\frac{2}{3}$ was no longer observable in the separation and reattachment regions.

REFERENCES

1. A. B. WITTE and E. Y. HARPER, Experimental investigation of heat-transfer rates in rocket thrust chambers, *AIAA Jl* **1**(2), 443–451 (1963).
2. L. H. BACK, P. F. MASSIER and H. L. GIER, Convective heat-transfer in a convergent–divergent nozzle, *Int. J. Heat Mass Transfer* 7(5), 549–568 (1964).
3. L. H. BACK, P. F. MASSIER and R. F. CUFFEL, Flow phenomena and convective heat transfer in a conical supersonic nozzle, *J. Spacecraft Rockets* 4(8), 1040–1047 (1967).
4. R. A. SEBAN, A. EMERY and A. LEVY, Heat transfer to separated and reattached subsonic turbulent flows obtained downstream of a surface step, *J. Aero/Space Sci.* **26**, 809–814 (1959).
5. R. A. SEBAN, Heat transfer to the turbulent separated flow of air downstream of a step in the surface of a plate, *J. Heat Transfer* **86**(2), 259–264 (1964).
6. E. G. FILETTI and W. M. KAYS, Heat transfer in separated, reattached and redevelopment regions behind a double step at entrance to a flat duct, *J. Heat Transfer* **89**(2), 163–168 (1967).

Résumé—On présente des mesures d'écoulement et de transport de chaleur pour de l'air chauffé s'écoulant à vitesse subsonique à travers un rétrécissement relié par un tube à un conduit conique. Ces mesures couvraient une gamme de rapports de températures de paroi à la température d'arrêt T_w/T_{to} allant de $\frac{1}{3}$ à $\frac{2}{3}$, et de nombres de Reynolds allant de 2×10^4 à 2×10^5, avec des données obtenues pour des couches limites laminaire et turbulente. On a fait également des mesures dans le cas d'un écoulement d'air non chauffé. Le champ d'écoulement de base établi à partir des mesures le long de la paroi et de la ligne des centres consiste en une déviation de l'écoulement à travers le conduit convergent qui produit un gradient de pression contraire (décélération) le long de la paroi. Les résultats de la visualisation de l'écoulement indiquent que celui-ci décollait juste en amont du conduit convergent courbe et se rattachait près de son extrémité. Les coefficients de transport de chaleur atteignaient une valeur minimale près du centre de la région de décollement, augmentaient au voisinage du point de rattachement, restaient constants dans le région de rattachement et réaugmentaient alors en aval. A cause de la section courbe et des effets associés au décollement de l'écoulement, le transport de chaleur dans la région décollée a été réduit, dans certaines conditions opératoires, en dessous des valeurs mesurées en amont dans le tube. Les valeurs du coefficient de transport de chaleur étaient plus élevées avec des couches limites minces produites par une longueur amont courte et refroidie, et la distribution du coefficient de transport de chaleur dans la région de rétablissement dépendait du fait que la couche limite est turbulente ou laminaire. Les effets du refroidissement de la paroi sous la forme de T_w/T_{to} qui ont été trouvés en amont dans le tube n'éraient pas observables dans les régions du décollement et du rattachement.

Zusammenfassung—Es werden Strömungs- und Wärmeübergangsmessungen wiedergegeben für Unterschallströmung von erhitzter Luft durch ein sich verengendes Übergangsstück, dass ein Rohr mit einem konischen Teil glatt verbindet. Die Messungen überspannen einen Bereich des Temperaturverhältnisses T_w/T_{to} (Temperatur der gekühlten Wand zu Ruhetemperatur) von $\frac{1}{3}$ bis $\frac{2}{3}$ und der Reynolds-Zahlen von 2×10^4 bis 2×10^5 mit Daten für laminare und turbulente Grenzschichten. Auch wurden Messungen ohne Erhitzung der Luft gemacht. Das grundsätzliche Strömungsfeld, wie es aus Messungen längs der Wand und längs der Kanalachse ermittelt wurde, zeigt eine Umkehrzone in der Strömung durch das sich verengende Übergangsstück, wodurch sich ein nicht erwarteter Druckanstieg (Verzögerung) längs der Wand ergibt. Eine Sichtbarmachung der Strömung zeigte, dass sich die Grenzschicht dicht vor der gekrümmten Kontur des Übergangsstückes ablöst und etwa an dessen Ende wieder zum Anliegen kommt.

Der Verlauf der Wärmeübergangskoeffizienten erreichte etwa in der Mitte der Ablösungszone ein Minimum, stieg mit Annäherung an den Punkt, wo die Strömung wieder anliegt, verlief dann in der Zone des Wiederanlegens ziemlich flach und wuchs stromabwärts schliesslich wider an. Als Folge der gekrümmten Kontur und der damit verbundenen Ablösungserscheinungen war der Wärmeübergang in der Ablösungszone unter bestimmten Versuchsbedingungen niedriger als die Werte, die stromaufwärts im Rohr gemessen wurden. Die Werte des Wärmeübergangskoeffizienten wurden höher bei dünnen Grenzschichten, die durch ein vorgeschaltetes, kurzes, gekühltes Rohrstück erzeugt wurden; der Verlauf des Wärmeübergangskoeffizienten in der Zone des Wiederanlegens der Strömung hing davon ab, ob die Grenzschicht turbulent oder laminar war. Auswirkungen der Kühlung der Wand in Abhängigkeit von T_w/T_{to}, wie sie stromaufwärts im Rohr festgestellt wurden, waren in der Zone des Ablösens und Wiederanlegens der Strömung nicht zu beobachten.

Аннотация—В статье представлены результаты измерений течения и теплообмена нагретого воздуха, движущегося с дозвуковой скоростью через сужение между цилиндрической трубой и коническим сечением. Эти измерения связали данные в диапазоне отношений охлажденная стенка-критическая температура T_w/T_{to} от $\frac{1}{3}$ до $\frac{2}{3}$, числа Рейнольдса от 2×10^4 до 2×10^5 с данными, полученными для ламинарного и турбулентного пограничных слоев. Производились также измерения ненагретого воздушного потока. Поле основного потока, установленное в результате измерений вдоль стенки и линии центра, расположено в области прохождения потока через сужение, в результате чего возникает обратный градиент давления. Результаты визуализации потока показали, что поток отрывается как раз выше по течению от изогнутого участка сужения и вновь присоединяется у его конца. Коэффициенты теплообмена достигают минимального значения у центра зоны отрыва, возрастают вблизи точки присоединения, выравниваются в области присоединения и затем снова возрастают вниз по потоку. Благодаря изогнутому участку и связанными с ним эффектами оторвавшегося потока, интенсивность теплообмена в зоне отрыва при определенных рабочих условиях падала ниже значений, измеренных вверх по потоку в трубе. Значения коэффициента теплообмена были выше при наличии тонких пограничных слоев, создаваемых коротким охлаждаемым участком вверх по потоку, а распределение коэффициента теплообмена в области переразвития зависело от того, был ли слой турбулентным или ламинарным. Эффекты охлаждения стенки, выраженные отношением T_w/T_{to}, обнаруженные вверх по потоку в трубе, не наблюдались в зонах отрыва и присоединения.